JOURNAL OF AIRCRAFT
Vol. 40, No. 6, November–December 2003

# Experimental Investigation of Corotating Vortex Filaments in a Water Tunnel

Kamran Rokhsaz* and Linda K. Kliment†
*Wichita State University, Wichita, Kansas 67260-0044*

**The dynamic behavior of corotating vortex filaments is investigated in a water tunnel. Comparisons are made between the motion of a single filament and that resulting from interactions between two filaments. Correlation is observed visually between the merger location and the vortex strength. In most cases vortex merger is shown to occur within one orbit. Quantitative data are presented on the variations of the vortex span, the amplitude of motion, the spiraling rate, and the center of spiraling, all as functions of downstream distance. It is shown that the vortex span does not vary considerably except in cases where the interactions among the filaments are strong. The amplitude of motion is shown to be much larger than that of a single vortex, while growing with downstream distance. Furthermore, the amplitude of motion is shown to exhibit a preferred direction in some cases. The presented data reveal that in the two-vortex cases the spiraling rate is nearly constant. It is also shown that despite considerable motion of the filaments the center of spiraling does not deviate significantly from a straight line.**

## Nomenclature

| | | |
|---|---|---|
| $b$ | = | blade separation distance |
| $b_v$ | = | vortex separation distance |
| $I_{\max}$, $I_{\min}$ | = | principal moments of inertia |
| $I_{xx}$, $I_{yy}$, $I_{zz}$ | = | moments of inertia |
| $L$ | = | distance downstream of the $C/4$ point |
| $r$ | = | radial distance from the mean vortex position |
| $\dot{r}$ | = | radial velocity |
| $U$ | = | freestream velocity |
| $V_y$, $V_z$ | = | velocity components of vortex motion |
| $x$, $y$, $z$ | = | coordinate axes |
| $x_c$, $y_c$, $z_c$ | = | centroid coordinates |
| $\alpha$ | = | angle of attack |
| $\Gamma$ | = | vortex strength |
| $\theta$ | = | angular position viewed from downstream |
| $\theta_p$ | = | inclination angle of the principal axes |
| $\omega$ | = | spiraling rate |

## Introduction

THE problem of aircraft wake vortex hazard became of critical importance with the advent of heavy transport aircraft. These aircraft operate within the terminal areas along with much lighter aircraft, which can be dangerously upset by the wake vortex system of the heavier vehicles. The issue is exacerbated by the fact that the vortex strength in the wake is not only linearly proportional to the aircraft weight, but also inversely proportional to flight speed. Furthermore, aircraft configured for takeoff and landing rely on much more complex high lift systems that result in generating several pairs of trailing vortices, the strongest of which could combine into a single pair at several span lengths downstream of the aircraft. Therefore, the safety problems associated with the air transport are manifested directly as aircraft-vortex encounters with a wide range of consequences. The current approach to preventing these problems consists of avoidance, which is becoming increasingly difficult with the rise in traffic congestion. An alternative approach is either eliminating the vortex wake or reducing the danger posed by it. A better understanding of the dynamics of the wake vortex system is required to make either one of these options feasible.

In 1970 Crow[1] offered an explanation for a form of dynamic instability that could lead to wake vortex breakdown. This instability, which results from the dynamic interaction of a single pair of vortex filaments driven by mutual induction effects, has been observed in atmospheric wake vortex degeneration events and in the laboratory.[2] In this analysis all vortices in the wake are assumed to have merged into two counter-rotating filaments.

Generally, the vortices shed by the tail and the fuselage wing junction are much weaker than those of the flap tip and the wing tip. Therefore, the former pair is either repelled or absorbed by the latter pair, slightly altering the location of the vortex merger.[3] Nonetheless, in most practical cases the corotating filaments emanating from the wing tip and the flap tip merge at some distance downstream to form a single strong vortex that poses the most danger to other aircraft. The interactions between the wing tip and the flap tip filaments before their merger have not received their due attention in the technical literature. This is especially true of the time-dependent motion of the filaments arising from mutual- and self-induction effects. Therefore, little is known about the influence of these phenomena on the location of vortex merger. The research presented in this document is an attempt to investigate some of these phenomena and their influence on vortex merger. However, prior to discussing the present investigation a brief review of the literature and different approaches in modeling the flow are in order.

### Two-Dimensional Analytical Models

Two-dimensional analytical models have been employed to gain insight into the behavior of three-dimensional wake, with the understanding that these models do not include effects such as Crow instability. However, these models have been useful in describing visually observed phenomena. For example, Greene[4] developed a model for predicting the effects of density stratification on wake motion and decay. It was found that wake lifetimes decrease in the presence of strong density stratification, turbulence, or a combination of the two. These analytical predictions of wake decay were in agreement with wake decay observations.

A number of analytical investigations were carried out to determine when and if corotating vortices would merge for a given configuration. Although experimental work indicated that merger does occur, some numerical analyses predicted that vortices might never merge in certain cases.[5] Other analytical cases determined merger of corotating vortices to be dependent on the initial conditions, such as

Presented as Paper 2002-3303 at the AIAA 32nd Fluid Dynamics Conference, St. Louis, MO, 24–26 June 2002; received 9 September 2002; revision received 25 February 2003; accepted for publication 6 March 2003. 

*Associate Professor, Department of Aerospace Engineering. Associate Fellow AIAA.
†Graduate Research Assistant, Department of Aerospace Engineering. Student Member AIAA.

distributed noise and small departures from symmetry.[6] These initial conditions were shown to change the interaction processes and lead to merger. Basu[7] showed that noise could accelerate merging and reduce the time needed for merger in a nearly linear fashion with increasing noise level. However noise did not seem to account for the discrepancies between experimental measurements of the time required for merger because the level of noise required for affecting that time proved to be higher than what could be found in wind tunnels or water tanks. These discrepancies could be legitimately questioned considering the large differences between the predicted times for merger. In fact, some analytical cases[6] showed merging to occur even after four orbits, whereas other studies[7] predict merger within one period.

Saffman[8] analyzed interaction and merger of viscous cores of uniform vorticity. He showed the merger to occur when the core radii exceed approximately a quarter of the distance separating their centroids. This result was verified experimentally by Meunier and Leweke.[9]

Regardless of the useful information they yield, all two-dimensional models lack the capacity to fully describe the behavior of three-dimensional wakes that contain additional degrees of freedom.

### Two-Dimensional Computational Models

Computational solutions offer the advantage of including all nonlinear effects in the equations of motion without many simplifying assumptions. Euler and Navier–Stokes methods can be used to model vortex flow, as well as the interaction of shocks and vortices.[10] A method used by Bilanin et al.[3] was shown to be suitable for solving the equations of motion through a second-order turbulent closure model of the Reynolds-stress equations. Unlike previous inviscid models, this formulation predicted viscous wake interactions. Hoeijmakers[10] found the number, the strengths, and the initial positions of the vortices trailed from a wing to be dependent on the spanwise lift distribution. It was also found that the least hazardous wake was generated when a flap and wing-tip vortex of the same sign and the same strength were shed from each wing.

Staufenbiel and Vitting[11] developed a computational method, based on the Biot–Savart approach, for the time-dependent roll-up process. The method revealed that the vortex core radius grows as downstream distance from the wing increases. This result was also confirmed with laser Doppler velocimetry measurements made in a water tunnel.

### Three-Dimensional Experimental Models

In the 1970s the three-dimensional interactions among multiple vortex filaments were studied experimentally with the emphasis placed on the far-field behavior of the wake. These studies focused on the wakes of individual aircraft configurations rather than on the standard behavior of interacting vortex filaments.[12–14] Corsiglia and Dunham[12] and Tymczyszyn and Barber[13] found that changing the span lift distribution on the wing can lead to a more rapid dissipation of the vortex system. However, the aircraft configurations required in a terminal control area (extended landing gear, reduced aircraft thrust, and aircraft sideslip) make this solution impractical. Further investigation illustrated that deflecting only the inboard flaps was effective in dispersing wake vorticity.[14] This configuration led to reduced rolling moments imposed on following aircraft.

More recently, Jacob and Savas[15] and Jacob[16,17] presented the results of their experimental investigations of the dynamic behavior of corotating vortex filaments. The authors conducted most of their studies in tow tanks using particle image velocimetry for flow measurements. They also conducted some wind-tunnel tests, where flow measurement was accomplished using a five-hole probe. A number of flap span ratios and the effect of Reynolds number on the merger of the two filaments were investigated. Their results indicated that the merger generally occurs within one orbit, except at higher Reynolds numbers. Although these studies resulted in better understanding of the details of these flowfields, they shed no light on the dynamics of the time-dependent motion of the filaments prior to their merger. Furthermore, in many cases the authors used wings with flaps to generate the corotating vortices. Consequently, the flowfield under consideration contained four vortex filaments. Therefore, the induced velocities of the other pair also influenced the behavior of the corotating filaments that were scrutinized.

As with two-dimensional analyses, three-dimensional experiments have yielded several solutions for the distance to merger. Bertenyi and Graham[18] suggested that the merging process takes longer to complete if the two vortices are of different strengths than in the case of vortices of equal strength. However, Chen et al.[19] observed that all corotating vortex pairs merge at about 0.8 orbit periods, regardless of the strengths of the vortices. Furthermore, Jacob[16] observed merger to occur at anywhere from $\frac{1}{4}$ to $\frac{1}{3}$ of an orbit period for typical cases, except at high Reynolds numbers.

The prevailing view is that a corotating vortex pair can be treated as a two-dimensional system, which should not merge unless the vortex cores are sufficiently large.[19] Using a simple vortex blob numerical simulation method, Bertenyi and Graham[18] showed the merging process to be essentially two-dimensional and inviscid. In some cases[9,20] the experimental data compared favorably with numerical solutions in that merger was shown to take place when the core radii become larger than approximately a quarter of the distance separating their centroids. Furthermore, Meunier and Leweke[9] showed that at low Reynolds numbers the vortices remain two-dimensional and merge into a single one. However, at higher Reynolds numbers the final vortex after merger is turbulent because of a three-dimensional instability. Merging was also shown by Brandt and Iversen[21] to take place even at larger vortex separation distances than predicted in earlier two-dimensional inviscid calculations. This behavior indicated that viscosity and possibly three-dimensional effects are important factors in the merging event.

### Three-Dimensional Analytical/Computational Models

Analysis of the wake-turbulence problem is complicated even though the equations of motion are known. Spalart[22] indicated that in order to describe the vortices realistically relatively small components such as the landing gear need to be included in the model. It is also difficult to specify the external factors (winds, atmospheric turbulence, and density stratification), which are required to describe the downstream wake dynamics.

In 1975 Jimenez[23] arrived at a model, very similar to that of Crow,[1] for analyzing the stability of a corotating vortex filament pair. He classified the modes of motion into symmetric and antisymmetric and showed both to be neutrally stable for all long wavelengths. In 1996 Crouch[24] presented a similar theoretical model predicting the motion of four vortex filaments. The results showed symmetric instabilities that are linked to the long-wavelength Crow instability. Symmetric and antisymmetric instabilities were observed at shorter wavelengths. Rennich and Lele[25] demonstrated similar results using direct numerical simulation.

There is also evidence that trailing vortices can be altered to some degree by various means,[26–28] including methods that use merger for reducing the threat of the wake vortex. Whether these methods can significantly impact a full-scale wake to the required level is still in question.[29] Vortex formation and development involves many parameters. It is not known at this time if alleviation is possible.

### Contribution of the Present Work

In the present paper the authors report on their experimental investigations of the time-dependent interactions of pairs of corotating vortex filaments. Measurements are made in a water tunnel using a light sheet to illuminate the vortex cross sections. The amplitude of motion is recorded, and its evolution is compared with that from the self-induced motion of a single filament. The authors believe that the understanding of the time-dependent motion is critical in that it can determine the distance over which the vortices merge.

## Experimental Approach

The experimental apparatus used for this research was identical to that described by Rebours[29] and Rebours et al.[30] A brief description of the equipment and the facility is given here. However, the reader is encouraged to consult Refs. 29 and 30 for further details.

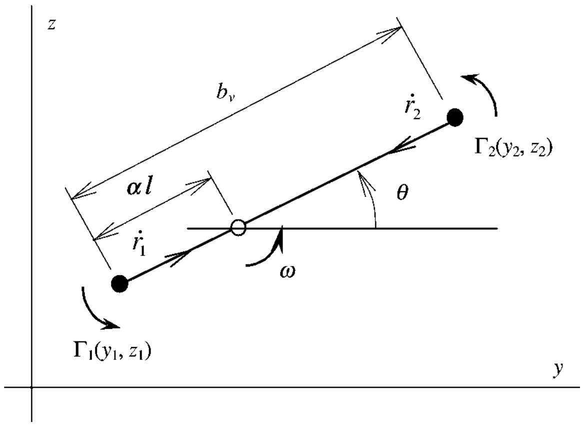


**Fig. 1 Schematic view of the spiraling vortices as seen from downstream.**

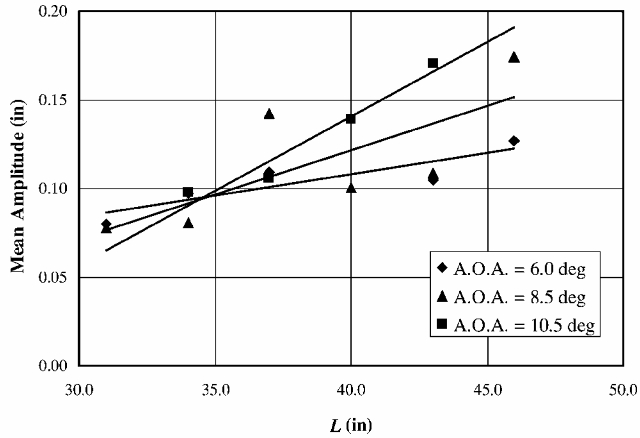


**Fig. 2 Mean amplitude of motion of the single vortex.**

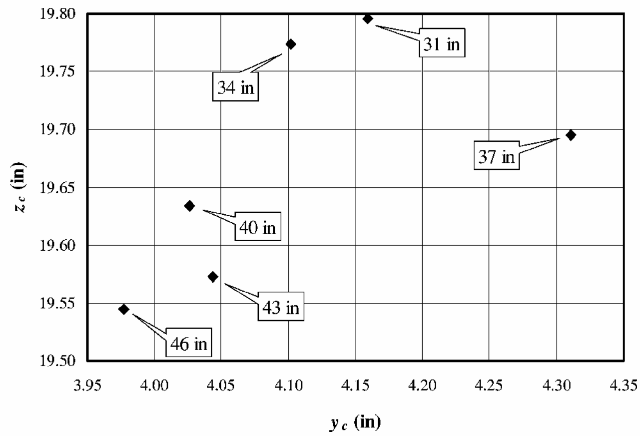


**Fig. 3 Time-averaged mean vortex position of a single vortex: $\alpha = 10.5$ deg.**

The test facility consisted of a water tunnel, in which a single or a pair of corotating vortex filaments were generated, near the entrance to the test section, using two flat blades. The blades could be positioned at arbitrary separation distances, controlling the vortex span, while varying their angles of attack allowed manipulating vortex strengths. The dynamics of these filaments were studied downstream of the generation point in the test section. The experimental method used for this research could not yield the filament strength in the single-vortex cases. Therefore, for this purpose the authors relied on the data of Ref. 31.

In the two-filament cases the vortex strengths were determined from the kinematics of the flow. Between every two downstream positions, for each filament the velocity of the mean vortex position could be approximated from its displacement. Then, from Fig. 1

$$V_{1,y} = \omega a b_v \sin\theta + \dot{r}_1 \cos\theta \tag{1}$$

$$V_{1,z} = -\omega a b_v \cos\theta + \dot{r}_1 \sin\theta \tag{2}$$

$$V_{2,y} = -\omega(1-a) b_v \sin\theta - \dot{r}_2 \cos\theta \tag{3}$$

$$V_{2,z} = \omega(1-a) b_v \cos\theta - \dot{r}_2 \sin\theta \tag{4}$$

The left-hand sides were measured experimentally, allowing for the solution of these equations for the radial and angular velocities and the location of the center of rotation. Consequently,

$$\Gamma_1 = 2\pi b_v^2 \omega (1-a) \tag{5}$$

and

$$\Gamma_2 = 2\pi b_v^2 \omega a \tag{6}$$

## Results and Discussion

### Single-Vortex Cases

For the purpose of comparison, several single-vortex cases were considered first. The water speed was set at 0.27 ft/s in every case, which corresponded to one of the lowest levels of background turbulence. The angle of attack was set at 6, 8, and 10.5 deg, and measurements were taken at downstream distances from 31 to 46 in. in 3-in. increments. The resulting data established a baseline for comparing the amplitude of motion of the two-vortex case. It also provided a measure of the level of fidelity of the data-acquisition method used for this study.

The average amplitude of motion at each downstream location was confined to less than one core diameter in every case. Foster[31] showed the latter quantity to be between 0.6–1.2 in. Furthermore, the amplitude grew with increasing distance downstream of the blade, but always remained less than one core diameter, as shown in Fig. 2. There was a larger spread in the results for angle of attack of 8.5 deg than for the other two cases shown in this figure. However, because this case was in between the other two cases it was considered justified to use a linear fit for this case as well.

Likewise, the mean vortex position did not change significantly from one downstream position to another. The displacements of the mean position remained within one core radius and appeared to be random. A typical case is demonstrated in Fig. 3. These data indicated that the wall interference was negligible, rendering the single vortex reasonably stationary within the length of the test section.

The frequency of vortex motion relative to its mean position at any one downstream location followed the same pattern as identified by Foster.[31] The Fourier transform of the data indicated that the majority of energy associated with this motion was concentrated at the low end of the frequency spectrum. The noise inherent in the data-acquisition method used for this research prevented resolution of the frequencies with great certainty. This was especially true in those cases where the amplitude of motion was much smaller than the core diameter. Furthermore, because the sample rate was limited by the frame rate of the camera, frequencies higher than 15 Hz could not be resolved. Nonetheless, results obtained in the course of this research were very consistent with those of Foster,[31] who used constant temperature anemometry.

The movements of the mean vortex position between the downstream location did not appear to follow a discernable pattern. Therefore, no frequency (wave number?) could be identified for the deviation of the filament from a straight line. Again, Foster[31] and Devenport et al.[32] reported a similar wandering behavior.

### Two-Vortex Cases

Tables 1 and 2 show the combination of the parameters used for the two-vortex cases. Strong interaction between the two filaments prevented quantitative data acquisition very far downstream or for very small blade separation distances. Nonetheless, in these cases the vortex-vortex interaction could be examined visually. Therefore, the cases considered for this study were divided into two groups. The

**Table 1 Two-vortex test matrix for visual observations**

| Case no. | $b$, in. | $\alpha_{Left}$, deg[a] | $\alpha_{Right}$, deg[a] |
|---|---|---|---|
| 1.1 | 1.0 | 11.0 | 11.5 |
| 1.2 | 1.0 | 9.0 | 9.5 |
| 1.3 | 1.0 | 7.5 | 7.5 |
| 1.4 | 1.0 | 6.0 | 6.0 |
| 1.5 | 1.0 | 4.5 | 4.5 |
| 1.6 | 1.5 | 10.5 | 11.0 |
| 1.7 | 1.5 | 9.5 | 9.0 |
| 1.8 | 1.5 | 7.0 | 7.5 |
| 1.9 | 1.5 | 6.0 | 6.0 |

[a]Left and right blades as viewed from downstream.

**Table 2 Two-vortex test matrix for quantitative data acquisition**

| Case no. | $b$, in. | $\alpha_{Left}$, deg[a] | $\alpha_{Right}$, deg[a] |
|---|---|---|---|
| 2.1 | 2.0 | 5.0 | 6.0 |
| 2.2 | 2.0 | 9.0 | 10.0 |
| 2.3 | 3.0 | 5.5 | 6.0 |
| 2.4 | 3.0 | 9.5 | 10.0 |
| 2.5 | 2.0 | 10.0 | 9.0 |
| 2.6 | 3.0 | 6.0 | 10.0 |

[a]Left and right blades as viewed from downstream. $L =$ 31, 34, 37, 40, 43, and 46 in.

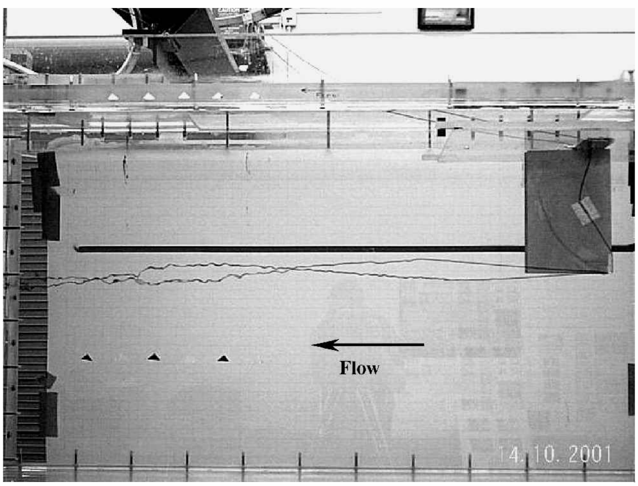


**Fig. 4 Typical view of the spiraling filaments in the test section: case 1.7.**

first group, represented in Table 1, consisted of those cases where only visual observations could be made. In these cases, the angles of attack were chosen to result in nearly equal vortex strength. The second group, shown in Table 2, were those in which quantitative data acquisition was possible. In the first four cases the vortex strengths were nearly equal. However, for the last two cases angles of attack were chosen such that the vortex strengths differed substantially.

*Visual Observations*

The merger location could be visually identified with reasonable certainty for nearly all of the cases considered in Table 1. However, at blade separations distances of 2 in. and larger, shown in Table 2, the filaments merged anywhere from a short distance beyond the end of the test section to the end of the tunnel, which prevented quantitative measurement of the merger location. Therefore, the results discussed in this section were obtained visually only.

Figure 4 shows a typical view of the spiraling of corotating vortices for blade separation of 1.5 in. In most cases the merger appeared to occur around one orbit, consistent with earlier reports.[15–17] However, in a few cases, such as that shown in Fig. 4, the filaments did not merge until well past one orbit. Visual observations indicated

**Table 3 Vortex strength in two-filament cases**

| Case no. | $\Gamma_{Left}$, In.$^2$/s | $\Gamma_{Right}$, in.$^2$/s[a] |
|---|---|---|
| 2.1 | 1.883 | 2.105 |
| 2.2 | 3.290 | 2.314 |
| 2.3 | 2.932 | 3.753 |
| 2.4 | 5.246 | 4.567 |
| 2.5 | 6.322 | 0.900 |
| 2.6 | 1.879 | 4.836 |

[a]Left and right as viewed from downstream.

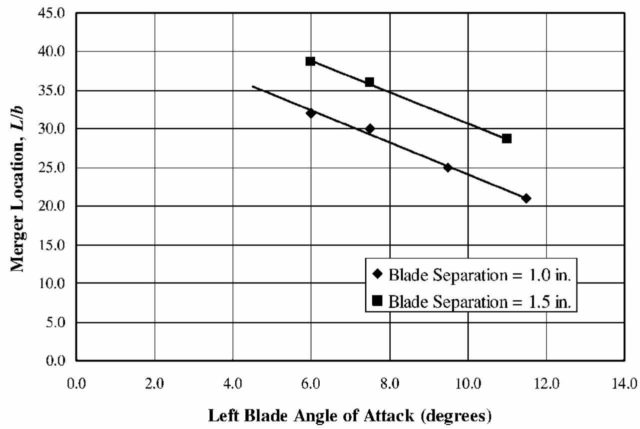


**Fig. 5 Visually observed vortex merger location.**

a clear relationship between the vortex strength and the merger location, as also indicated in Fig. 5. In the absence of a method to measure the vortex strength reliably, the left-blade angle of attack was used in this figure to show this correlation. This figure indicates that stronger vortices or stronger interaction between the filaments (i.e., shorter distance between the blades) resulted in their earlier merger downstream of the blades. Again, the reader is cautioned that these observations were limited to cases where the two vortices were of approximately the same strength.

*Quantitative Observations*

For the blade separation distances shown in Table 2, quantitative data acquisition was possible. Therefore, these results could be compared directly with those from the single-vortex cases. Vortex strengths were estimated using Eqs. (1–6) and are shown in Table 3. In the absence of other data for verification, these values could be compared with those for single-filament cases of Foster.[31] Such comparison indicated the estimated vortex strengths to be in the expected range. Nonetheless, the individual vortex strengths were not used for any purpose other than to indicate the relative strengths of the two filaments.

Vortex span was defined as the direct distance between the time-averaged mean position of the filaments. The variation of this quantity as a function of downstream position is shown in Fig. 6 and 7 for the six cases shown in Table 2. Results shown in these figures indicated that the vortex span did not vary significantly for the larger blade separation distance, regardless of the vortex strength. This trend might be significant in that no vortex merger was observed in these cases within the uniform-flow section of the tunnel. However, the combination of the large and comparable vortex strengths and small blade separation distance resulted in a rapidly decreasing vortex span downstream of the blades, as shown in Fig. 6. This behavior pointed to the possible presence of a threshold for the level of vortex-vortex interaction, above which the filaments would attract each other.

The amplitude of motion was of interest as a function of time at fixed downstream locations. Furthermore, the trends associated with the mean amplitude as a function of downstream position could be compared with those of the single-vortex cases. Investigating the vortex movement at fixed downstream locations the following two observations could be made:

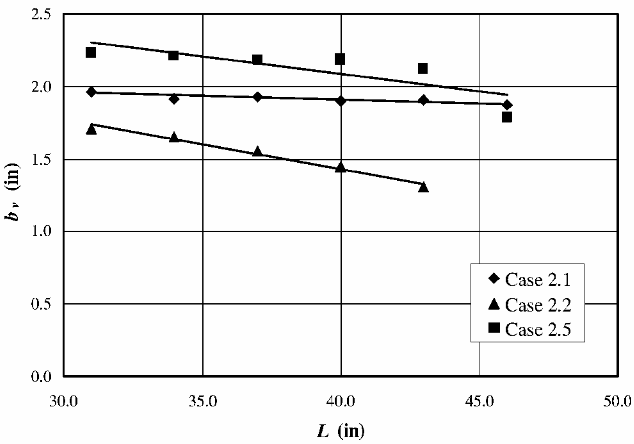


**Fig. 6 Vortex span as a function of downstream distance for 2-in. blade separation.**

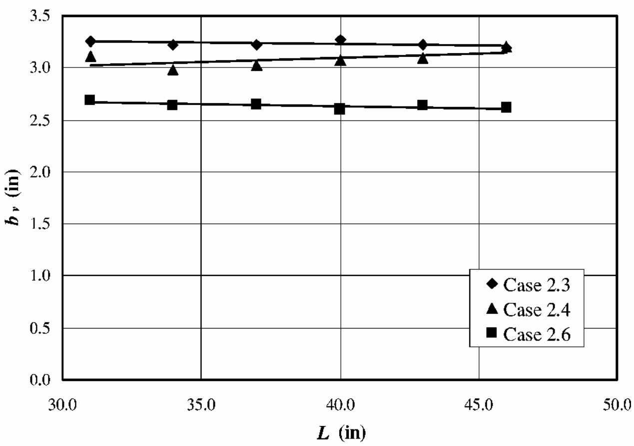


**Fig. 7 Vortex span as a function of downstream distance for 3-in. blade separation.**

1) In those cases where the filaments were of nearly equal strength, their amplitudes were also nearly equal, whereas in those cases where the strengths differed substantially the weaker vortex moved with a much larger amplitude.

2) In certain cases the amplitude of motion appeared to favor one direction. At this writing, no correlation has been established between the vortex strength and this behavior. It is also noteworthy that this observation was contrary to that implied by Jimenez.[23]

Figures 8 and 9 represent examples of typical core positions at fixed downstream distances. The reader is reminded again that in these figures the words left and right refer to the location of the blade that generated the vortex.

In Fig. 8a it is visually obvious that each vortex moved with equal amplitude in all directions. However, even in this case a direction could be established in which the vortex preferred moving. Constructing histograms for the components of displacement along this direction and normal to it resulted in nearly equal probability of motion along each axis. This behavior is shown in Figs. 8b and 8c.

Figure 9 is that of a case in which one of the vortices was significantly weaker. Visual inspection of Fig. 9a indicated that the weaker vortex moved with a larger amplitude. At the same time its preferred direction of motion was not along the line connecting the two vortices, nor was it perpendicular to that direction. Constructing histograms for the amplitudes of motion along the principal axes resulted in Figs. 9(b) and 9(c). It is quite evident from these figures that the vortices demonstrated a greater probability of moving along one of the axes.

The data presented in Figs. 8 and 9 show the probability of the vortices moving away from their time-averaged centroidal positions was nearly normal. The noise inherent in the data-acquisition

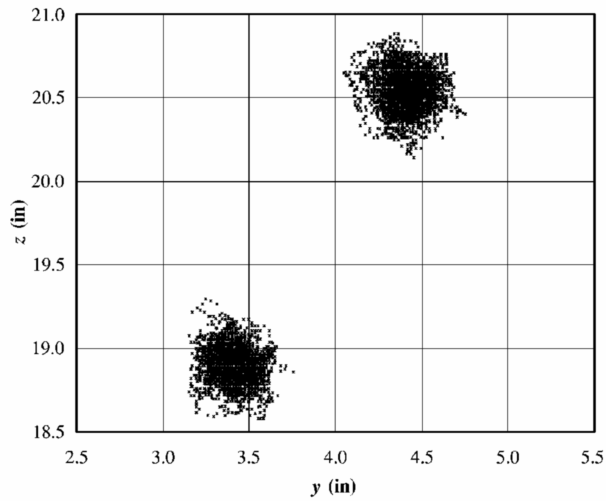


**a) Time exposure of the core position**

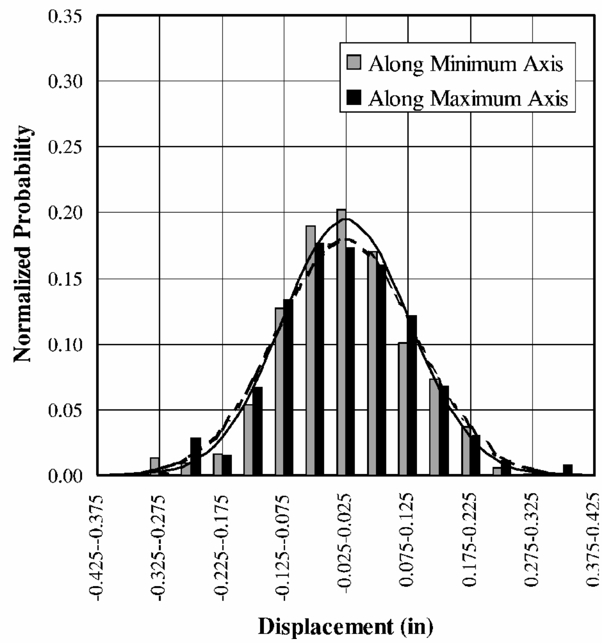


**b) Right vortex displacement histogram**

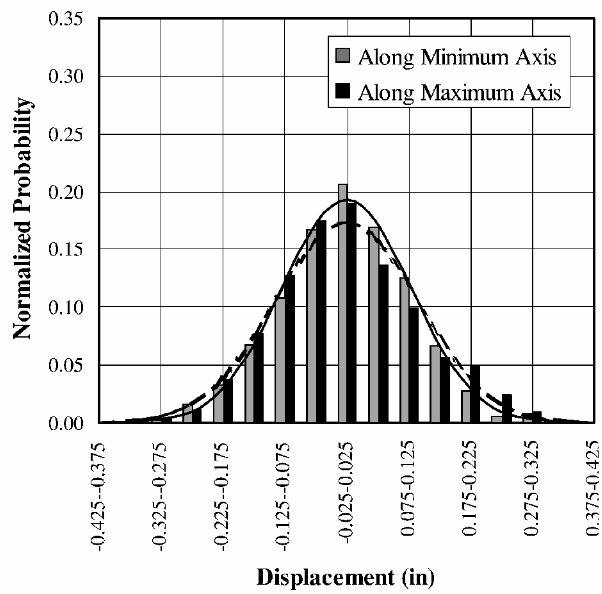


**c) Left vortex displacement histogram**

**Fig. 8 Behavior of vortex motion for case 2.1, $L = 37$ in.**

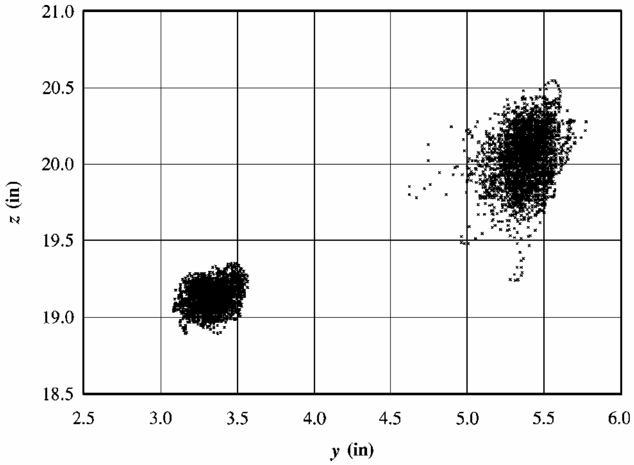


**a) Time exposure of the core position**

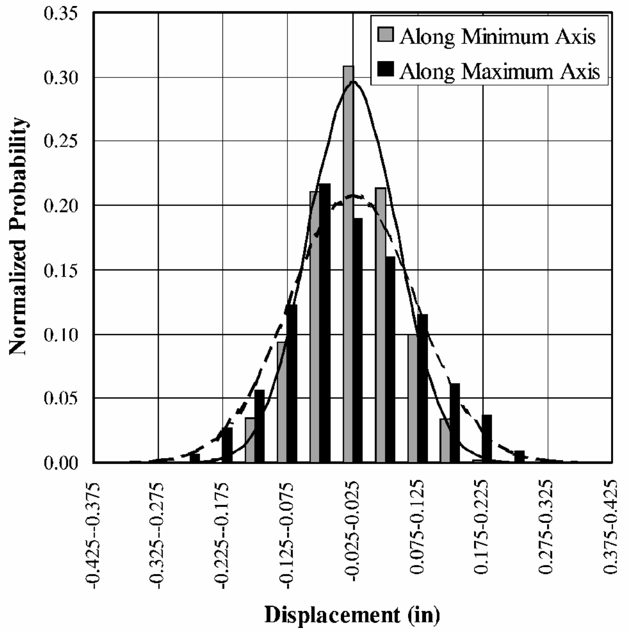


**b) Right vortex displacement histogram**

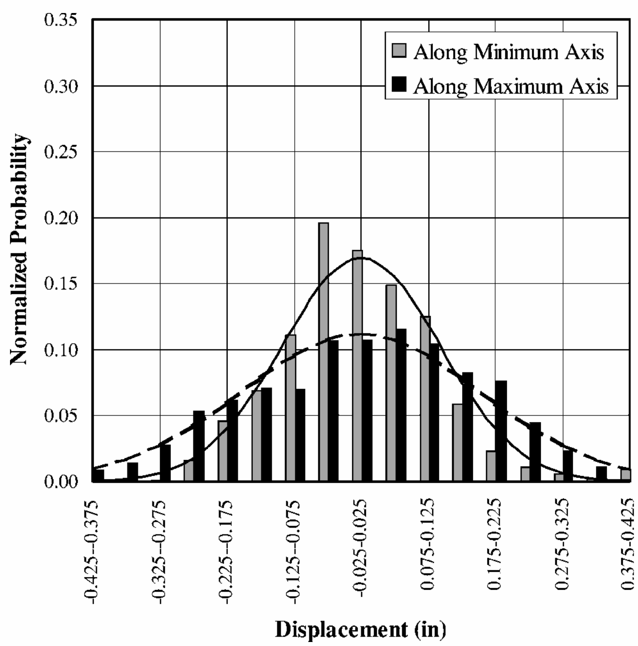


**c) Left vortex displacement histogram**

**Fig. 9 Behavior of vortex motion for case 2.5, $L = 31$ in.**

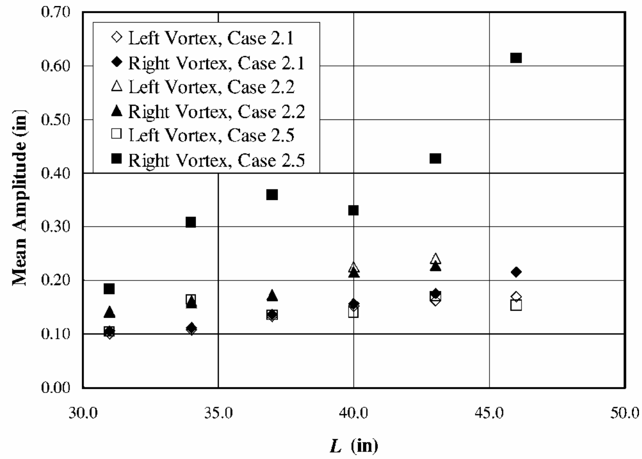


**Fig. 10 Mean amplitude of motion for the 2-in. blade separation.**

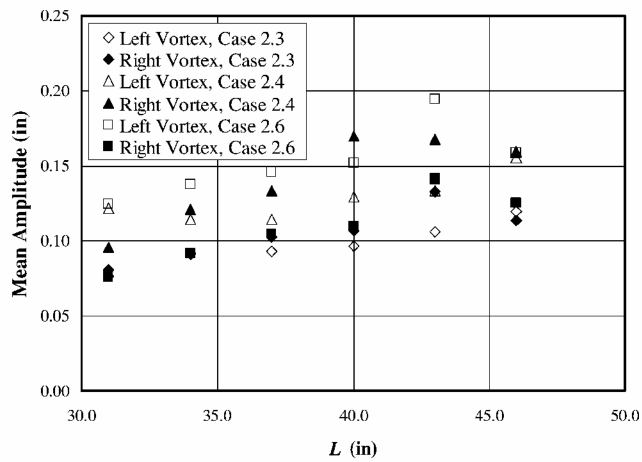


**Fig. 11 Mean amplitude of motion for the 3-in. blade separation.**

technique used here prevented any meaningful analysis of the frequency content of the motion.

Figures 10 and 11 show the mean amplitude of the vortex motion at various downstream locations. Unlike in the single-vortex cases, it was not obvious if the growth in the amplitude of motion shown in these figures followed a linear behavior with increasing downstream distance. Therefore, a linear fit of the data is not shown in these figures. However, it is evident from these figures that the amplitudes on both sides matched quite well as long as the two filaments were of comparable strength. Consistent with the observations made above, if one filament were noticeably weaker than the other, it moved with a much larger amplitude than the stronger filament. Furthermore, as in the single-vortex case, the amplitudes increased monotonically with downstream distance. However, the mean amplitude was much larger than that of the single vortex. The larger amplitude could be attributed to the interactions between the two filaments that became stronger with increasing vortex strength and with decreasing vortex span.

The spiraling of the two filaments was characterized with the change in the inclination angle of the straight line connecting them. Figures 12 and 13 show this inclination angle as a function of the downstream location. The slopes of these curves constituted the spiraling rate, which remained nearly constant in each case. Predictably, the reduction in the distance between the filaments, as well as the increase in the vortex strength, boosted the spiraling rate. This behavior indicated that the vortex strength generated by the blades was not only a function of the blade angle of attack, but also depended on the aerodynamic coupling between the blades.

Despite considerable motion of the filaments, the center of spiraling did not move significantly within the distance over which data were acquired. Figure 14 shows the downstream view of one of the cases considered in this study. The center of spiraling can be

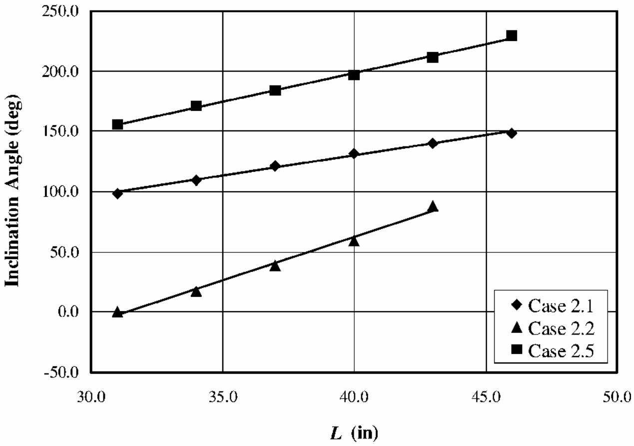


**Fig. 12 Vortex spiraling rate for the 2-in. blade separation.**

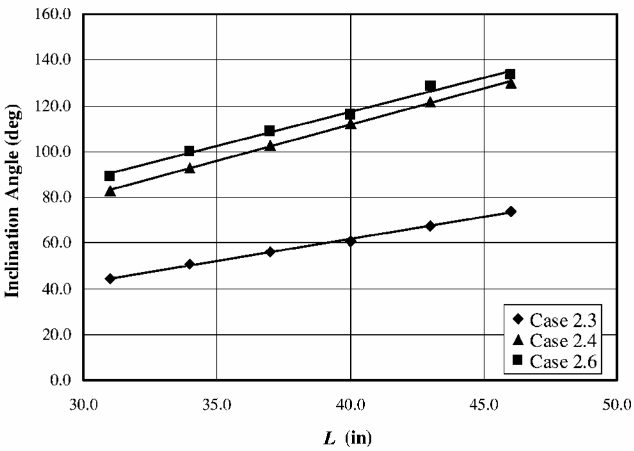


**Fig. 13 Vortex spiraling rate for the 3-in. blade separation.**

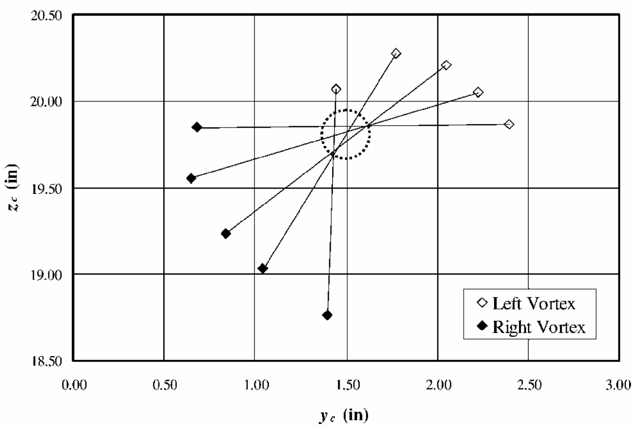


**Fig. 14 Downstream view of the spiraling vortex pair for case 2.2.**

approximately located from the intersections of the lines connecting the vortices. It is clear from this figure that these intersections remained confined to less than one core diameter (i.e., the circle marked by the dotted line). Furthermore, as with the single-vortex movement, the movement of the center of rotation between downstream locations seemed to be random.

## Conclusions

The interactions between pairs of corotating vortex filaments were studied in a water tunnel and compared with the motion of a single filament. Visual observations indicated a clear relationship between the vortex strength and the merger location. In most cases the merger occurred within one orbit, but that was not always the case.

Quantitative data acquisition was performed while varying vortex span and relative vortex strength, using a novel technique relying on video recordings of the vortex motion. The amplitude of motion, while growing with increasing downstream distance, was shown to be larger than that of a single filament. Time-averaged vortex spans were measured in a number of cases and shown to be nearly constant for weak vortices and for large blade separation distances. Furthermore, despite considerable motion of the filaments the center of spiraling did not move significantly within the distance over which data were acquired. The motion of the centroid of the single vortex and the center of rotation of the two-vortex cases appeared to be random, although with very small amplitudes.

Unlike the theoretical predictions, the two-vortex temporal motion showed a preferred direction in a number of cases. No correlation was established between absolute and relative vortex strengths and this tendency. Therefore, this phenomenon is recommended for further study.

## References

[1]Crow, S. C., "Stability Theory for a Pair of Trailing Vortices," *AIAA Journal*, Vol. 8, No. 12, 1970, pp. 2172–2178.

[2]Eliason, B. G., Gartshore, I. S., and Parkinson, G. V., "Wind Tunnel Investigation of Crow Instability," *Journal of Aircraft*, Vol. 12, No. 12, 1975, pp. 985–988.

[3]Bilanin, A. J., Teske, M. E., and Williamson, G. G., "Vortex Interactions and Decay in Aircraft Wakes," *AIAA Journal*, Vol. 15, No. 2, 1977, pp. 250–260.

[4]Greene, G. C., "An Approximate Model of Vortex Decay in the Atmosphere," *Journal of Aircraft*, Vol. 23, No. 7, 1986, pp. 566–573.

[5]Dritschel, D. G., "A General Theory for Two-Dimensional Vortex Interactions," *Journal of Fluid Mechanics*, Vol. 293, 1995, pp. 269–303.

[6]Caperan, P., and Verron, J., "Numerical Simulation of a Physical Experiment on Two-Dimensional Vortex Merging," *Fluid Dynamics Research*, Vol. 3, No. 1–4, 1988, pp. 87–92.

[7]Basu, A. J., "The Role of Noise in Two-Dimensional Vortex Merging," *Fluid Dynamics Research*, Vol. 10, 1992, pp. 169–180.

[8]Saffman, P. G., *Vortex Dynamics*, Cambridge Univ. Press, New York, 1997.

[9]Meunier, P., and Leweke, T., "Merging and Three-Dimensional Instability in a Corotating Vortex Pair," *Vortex Structure and Dynamics; Lectures of the Workshop, Rouen, France, April 1999*, edited by A. Maurel and P. Petitjeans, Springer-Verlag, Berlin, 2000, pp. 241–251.

[10]Hoeijmakers, H. W. M., "Modeling and Numerical Simulation of Vortex Flow in Aerodynamics," *AGARD Conference Proceedings 494: Vortex Flow Aerodynamics*, Vol. CP-494, North Atlantic Treaty Organization Advisory Group for Aerospace Research and Development, Neuilly sur Seine, France, 1990, pp. 1.1–1.46.

[11]Staufenbiel, R., and Vitting, T., "On Aircraft Wake Properties and Some Methods for Stimulating Decay and Breakdown of Tip Vortices," *AGARD Conference Proceedings 494: Vortex Flow Aerodynamics*, Vol. CP-494, North Atlantic Treaty Organization Advisory Group for Aerospace Research and Development, Neuilly sur Seine, France, 1990, pp. 26.1–26.14.

[12]Corsiglia, V. R., and Dunham, R. E., Jr., "Aircraft Wake Vortex Minimization by Use of Flaps," NASA SP-409, Feb. 1976, pp. 303–336.

[13]Tymczyszyn, J. J., and Barber, M. R., "Recent Wake Turbulence Flight Test Programs," *SETP 1974 Report to the Aerospace Profession—Eighteenth Symposium Proceedings*, Society of Experimental Test Pilots, Lancaster, CA, 1974, pp. 52–68.

[14]Corsiglia, V. R., Rossow, V. J., and Ciffone, D. L., "Experimental Study of the Effect of Span Loading on Aircraft Wakes," *Journal of Aircraft*, Vol. 13, No. 12, 1976, pp. 968–973.

[15]Jacob, J. D., and Savas, O., "Vortex Dynamics in Trailing Wakes of Flapped Rectangular Wings," AIAA Paper 97-0048, Jan. 1997.

[16]Jacob, J. D., "Experimental Investigation of Co-Rotating Trailing Vortices," AIAA Paper 98-0590, Jan. 1998.

[17]Jacob, J. D., "Experiments on Trailing Vortex Merger," A99-16426, AIAA Paper 99-0547, Jan. 1999.

[18]Bertenyi, T., and Graham, W., "An Experimental Study of the Merging of Aircraft Wake Vortices, " AIAA Paper 2000-4129, Aug. 2000.

[19]Chen, A. L., Jacob, J. D., and Savas, O., "Dynamics of Corotating Vortex Pairs in the Wakes of Flapped Airfoils," *Journal of Fluid Mechanics*, Vol. 382, 1999, pp. 155–193.

[20]Leweke, T., and Williamson, C. H. K., "Long-Wavelength Instability and Reconnection of a Vortex Pair," *IUTAM Symposium on Dynamics of Slender Vortices*, edited by E. Krause and K. Gersten, Kluwer Academic Publishers, Dordrecht, The Netherlands, 1998, pp. 225–234.

[21] Brandt, S. A., and Iversen, J. D., "Merging of Aircraft Trailing Vortices," *Journal of Aircraft*, Vol. 14, No. 12, 1977, pp. 1212–1220.

[22] Spalart, P. R., "Airplane Trailing Vortices," *Annual Review of Fluid Mechanics*, Vol. 30, 1998, pp. 107–138.

[23] Jimenez, J., "Stability of a Pair of Co-Rotating Vortices," *Physics of Fluids*, Vol. 18, No. 11, 1975, pp. 1580, 1581.

[24] Crouch, J. D., "Stability of Multiple Trailing-Vortex Pairs," *AGARD Conference Proceedings 584: The Characterisation and Modification of Wakes from Lifting Vehicles in Fluids*, Vol. CP-584, North Atlantic Treaty Organization Advisory Group for Aerospace Research and Development, Neuilly sur Seine, France, 1996, pp. 17.1–17.8.

[25] Rennich, S. C., and Lele, S. K., "Method for Accelerating the Destruction of Aircraft Wake Vortices," *Journal of Aircraft*, Vol. 36, No. 2, 1999, pp. 398–404.

[26] Rossow, V. J., "Prospects for Destructive Self-Induced Interactions in a Vortex Pair," *Journal of Aircraft*, Vol. 24, No. 7, 1987, pp. 433–440.

[27] Crouch, J. D., "Instability and Transient Growth for Two Trailing-Vortex Pairs," *Journal of Fluid Mechanics*, Vol. 350, 1997, pp. 311–330.

[28] Crouch, J. D., Miller, G. D., and Spalart, P. R., "Active-Control System for Breakup of Airplane Trailing Vortices," *AIAA Journal*, Vol. 39, No. 12, 2001, pp. 1–8.

[29] Rebours, R., "Quantitative Measurement of Wake Vortex Motion in a Water Tunnel," Master's Thesis, Dept. of Aerospace Engineering, Wichita State Univ., Wichita, KS, May 2001.

[30] Rebours, R., Kliment, L. K., and Rokhsaz, K., "Forced Response of a Vortex Filament Pair Measured in a Water Tunnel," AIAA Paper 2001-2448, June 2001.

[31] Foster, S. R., "Exploratory Study of an Aircraft Wake Vortex Filament in a Water Tunnel," Master's Thesis, Dept. of Aerospace Engineering, Wichita State Univ., Wichita, KS, Dec. 1999.

[32] Devenport, W. J., Rife, M. C., Liapis, S. I., and Follin, G. J., "The Structure and Development of a Wing-Tip Vortex," *Journal of Fluid Mechanics*, Vol. 312, 1996, pp. 67–106.